

Theoretical and Experimental Studies on Transversely Polarized Smectic Liquid Crystals

Thesis submitted to
Jawaharlal Nehru University
for the award of the degree of
Doctor of Philosophy

by

Arun Roy



**Raman Research Institute
Bangalore 560 080**

July, 1997



043:538.9 LC ROY

19821

DECLARATION

I hereby declare that this thesis is composed independently by me at the Raman Research Institute, Bangalore, under the supervision of Prof. N. V. Madhusudana. The subject matter presented in this thesis has not previously formed the basis of the award of any degree, diploma, associateship, fellowship or any other similar title in any other University.



(Prof. N. V. Madhusudana)

Raman Research Institute
Bangalore



(Arun Roy)

CERTIFICATE

This is to certify that thesis entitled **Theoretical and Experimental Studies on Transversely Polarized Smectic Liquid Crystals** submitted by **Arun Roy** for the award of the degree of DOCTOR OF PHILOSOPHY of Jawaharlal Nehru University is his original work. This has not been published or submitted to any other University for any other Degree or Diploma.



Prof. N. Kumar
(Centre Chairperson)

Director

Raman Research Institute



Prof. N. V. Madhusudana
(Thesis Supervisor)

Raman Research Institute

Contents

Acknowledgments	v
Preface	vii
1 Introduction	1
1.1 Liquid Crystals	1
1.1.1 Chiral molecules	2
1.1.2 Achiral molecules	3
1.2 Nematics	3
1.2.1 Nematic phase (N)	4
1.2.2 Chiral nematic or cholesteric phase (N*)	5
1.3 Smectics	5
1.3.1 Smectic A phase (SmA)	6
1.3.2 Smectic C phase (SmC)	6
1.3.3 Chiral smectic C phase (SmC*)	7
1.3.4 Chiral smectic C antiferroelectric liquid crystals	9
2 Phase transitions in Antiferroelectric Liquid Crystals: A Theoretical Model	13
2.1 Overview	13
2.2 Continuum theory of AFLC	15
2.2.1 Order parameters	16
2.2.2 Homogeneous case	17
2.2.3 Inhomogeneous case	19
2.3 Other relevant models	21
2.4 Discrete model of AFLC	24
2.4.1 Origin of inter-layer interactions	25
2.4.2 The discrete model	28
2.4.3 Calculations	29
2.4.4 Results and discussion	30
2.5 Conclusions	33

3	Electric field induced structures in antiferroelectric liquid crystals	35
3.1	Introduction	35
3.2	Electric field order parameter coupling	36
3.3	SmC* under a transverse electric field	37
3.4	Commensurate and incommensurate structures	40
3.4.1	Basic definitions	42
3.4.2	1-d Chiral xy model	44
3.5	AFLC under transverse electric field	45
3.6	Computational methods and difficulties	46
3.7	Field induced structures in AFLC	47
3.7.1	Structures in antiferroelectric phase	47
3.7.2	Structures in ferrielectric phases	50
3.7.3	Structures in SmC _α * phase	50
3.8	Calculation of apparent tilt angle	51
3.9	Results and comparison with experiments	51
3.10	Conclusions	54
4	Optical properties of antiferroelectric liquid crystals	55
4.1	Introduction	55
4.2	Berreman's 4 x 4 matrix method	60
4.3	Generating conosopic figures	62
4.3.1	What is conoscopy?	62
4.3.2	Simulating conosopic figures for AFLC	63
4.3.3	Comparison with experiments	67
4.4	Ellipsometry	69
4.4.1	General introduction	69
4.4.2	Calculation of ellipsometric parameters for AFLC thin films	70
4.4.3	Comparison with experiments	71
4.5	Optical rotatory power	75
5	An ANNNXY model for transversely polarized achiral smectics	77
5.1	Introduction	77
5.2	Theoretical model	80
5.3	Calculations and discussion	82
5.3.1	Effective potential method	82
5.3.2	Theoretical phase diagrams	84
5.3.3	Comparison with experiments	86
5.4	Conclusion	87
6	Electrooptic studies on AFLC	89

6.1	Introduction	89
6.2	Experimental	90
6.2.1	Electrooptic measurement setup	90
6.2.2	Samples used in the experiments	93
6.2.3	Sample cell preparation	94
6.3	Results and discussion	96
6.3.1	Homogeneous geometry	96
6.3.2	Homeotropic geometry	104
6.4	Conclusions	105
	Summary	107

Acknowledgments

Several people have helped me to make this thesis possible. I am most indebted to my thesis advisor Prof. N. V. Madhusudana. The guidance, encouragement and support from him has been invaluable in accomplishing this work. His intuitive insight in physics has been a great resource in my research.

From our research group, I owe many thanks to Dr. Pratibha, Dr. Y. Hatwalne, and Dr. V. A. Raghunathan for many valuable academic suggestions. I am also indebted to Prof. R. Nityananda and Prof. J. Samuel for teaching me some of the theoretical concepts at the early stage of my research career. I thank Prof. B. K. Sadashiva from Chemistry laboratory for providing us valuable information about the chemistry of liquid crystals.

I am thankful to Prof. N. Kumar, director of Raman Research Institute for his interest in my work.

I thank Ms. S. Sarala and Mr. K. Subramanya for all their help in conducting the experiments. I would also like to thank Mr. Mani, Mr. Nagaraj and Mr. Ram from liquid crystal workshop for providing their expertise and technical help in setting up the electrooptic measurement system.

I thank Prof. C. Destrade and Prof. H. T. Nguyen from the Centre de Recherche Paul Pascal (CRPP) Bordeaux, for providing us the samples which made electrooptic measurements possible.

I thank Prof. H. Takezoe from Tokyo Institute of Technology, Japan, for kindly sending us the preprints of their papers on bent banana shaped molecules. Without his timely response our work on this system would have been delayed.

I am thankful to Mr. S. Raghavachar and Mr. K. Radhakrishna for helping me in preparing the manuscripts of some of the papers and helping with administrative matters.

I have no words to thank all my friends for the numerous impacts they have made during the period of my research work. I am especially indebted to my colleagues Geetha Basappa, Sobha Warriar, P. A. Pramod and from outside the laboratory C. Indrani, Debnarayan Jana, Dipanjan Mitra and Andal Narayan for their help in both academic and non-academic life.

Without the facilities provided by our library this work would not have been possible. In particular, I am grateful to the library staff for providing me round the clock access to the library during the preparation of this thesis. I thank Mr. Ratnakar, Ms. Girija and their colleagues for their helpful attitude. I would also like to acknowledge the facilities provided by the computer section.

Finally, my deep gratitude to my parents, my brother and sister for their constant

moral support in pursuing this research career. Without their love and encouragement, I would not have known a single word about physics.

Preface

Organic rod like molecules forming liquid crystalline phases often carry permanent electric dipole moments. Therefore one may expect ferroelectric properties in these liquid crystalline phases. However, in most of the liquid crystalline phases, the symmetry is high and the molecules have a free rotation about their long axes and have an apolar distribution function of their long axes. As such, the phases are not ferroelectric. On the other hand if the molecules are chiral (*i.e.*, noncentrosymmetric), the symmetry of the resulting liquid crystalline phases, usually denoted by an asterisk, can get considerably reduced. A variety of phases consisting of chiral molecules have been discovered and studies on these phases form an active field of research. Meyer *et al.* [1] first demonstrated in 1975 that the symmetry of the layers in the chiral smectic-C (SmC^*) liquid crystals allows them to be polarized in the plane of the layers. Thus SmC^* liquid crystals constitute the first known example of a ferroelectric medium with liquid like order. Because of the linear coupling of an external electric field with the spontaneous polarization, which in turn is coupled to the tilt order of molecules within the layers, these materials have potential applications in display devices. A large number of compounds exhibiting the SmC^* phase have been synthesized and their properties are now well established.

In 1989 Chandani *et al.* [2, 3] discovered antiferroelectric properties in the lower temperature chiral tilted smectic phase of the compound MHPOBC. Further detailed studies reveal that this novel compound exhibits a rich variety of phases apart from the ferroelectric SmC_β^* and antiferroelectric SmC_A^* phases. The phase sequence exhibited by MHPOBC with decreasing temperature is:

Isotropic – SmA – SmC_α^* – SmC_β^* – SmC_γ^* – SmC_A^* – SmI_A^* – Crystal.

where SmA represents the smectic-A phase. In all the lower temperature *chiral* smectic-C phases, the average orientation direction of the molecules (the director A) is tilted with respect to the layer normal and \hat{n} has spontaneous helicoidal structure along the layer normal. The SmC_β^* is identified to be the usual ferroelectric SmC^* phase. In the SmC_A^* , the tilt directions of the director \hat{n} in successive layers are almost opposite and hence the polarizations, giving rise to the antiferroelectric properties of this phase. Though the structures of the SmC_β^* and SmC_A^* phases are known [4, 5], those of the SmC_γ^* and SmC_α^* phases are not yet clearly established. From the polarization measurements, SmC_γ^* phase is characterized as ferrielectric in nature as its polarization is less than that of the ferroelectric SmC_β^* phase. The SmC_α^* phase appears just below the stability range of the SmA phase and has a small tilt angle [6] and a very short pitch [7]. SmI_A^* represents a liexatic smectic-I* phase which also has antiferroelectric order. More than 300 compounds

are now known to exhibit the antiferroelectric SmC_A^* phase and the properties of these antiferroelectric liquid crystals (AFLC) are being studied in detail in several laboratories.

We started our investigations on AFLC to detect experimentally the subtle phase transitions exhibited by these compounds. As the medium is polarized, dielectric measurements have been extensively used to study the phase transitions in these compounds. The electroclinic effect in which an external electric field induces a tilt in the SmA phase has been a very useful method of exploring the critical soft mode in the SmA phase close to the SmA-SmC* transition point. The electrooptic response in the lower temperature tilted phases can also be expected to yield very useful information about the structures and dynamics in these phases. We conducted electrooptic measurements for two different geometries *viz.* homogeneous and homeotropic geometries of the sample. We found that all the transitions between the various sub-phases exhibited by these compounds could be very easily detected using this technique. We were able to measure an electrooptic effect, for the first time in the antiferroelectric and SmI_A^* phases of a tolane compound. We have observed a new electrooptic mode which has a relatively high relaxation frequency ($\gtrsim 100$ kHz) in the antiferroelectric SmC_A^* phase of the C8-tolane compound. We have argued that it can arise from the electroclinic soft mode which produces an asymmetric tilt in successive layers of the antiferroelectric phases.

Several other experimental studies using a variety of techniques have established the following facts:

- All the tilted phases have a helical structure and it is established by optical measurements that the sense of the helix is opposite in SmC_β^* and SmC_A^* phases [8].
- All the transitions between different tilted phases are *weakly* first order in nature as determined by differential scanning calorimetry (DSC) with heats of transition ~ 1 joule/mole [9].
- The stability of the SmC_α^* and ferrielectric phases is sensitive to the optical purity of the sample. The temperature ranges of stability of these phases decrease and finally go to zero when the compound is mixed with its opposite handed enantiomer [6]. The range of SmC_α^* phase shrinks as the nonchiral chain length is increased [9].
- The *ferrielectric* SmC_γ^* phase in several pure compounds consists of two ferri phases [9] whereas in some binary mixtures there are three sub-phases FI_H , SmC_γ^* and FI_L [6].
- The ferrielectric phase has a rather turbid appearance with in-plane birefringence rendering optical measurements in this phase difficult [10].
- Studies on several homologous series have shown a prominent *odd-even* effect in the phase transition temperatures between the SmC_β^* to SmC_γ^* as well as SmC_γ^* to SmC_A^* phases [9].
- A strong transverse dipolar group attached close to the chiral center favours the formation of the SmC_A^* phase. However, even racemic mixtures with zero polarization [6] and achiral compounds [11] also exhibit the *anticlinic* phase in which successive layers have opposite tilts.

- Switching current measurements reveal that the SmC_α^* phase has ferroelectric characteristics at lower temperatures but antiferroelectric characteristics close to the SmA-SmC_α^* transition temperature [12, 13].
- Measurements of the apparent tilt angle (the angle between the effective optical axis of the field distorted structure and the layer normal) on homogeneously aligned samples revealed that in the SmC_α^* phase, there is a step like variation of the apparent tilt angle as a function of an in-plane external static electric field [14]. This led to the speculation that there is a field induced *devil's staircase* in this phase.
- The variation of the apparent tilt angle with the applied dc electric field in the ferroelectric phase exhibits a plateau at one third of the tilt angle at intermediate fields [14].
- The conoscopic figures obtained from thick homeotropically aligned samples also show distinct characteristic changes as a function of an in-plane external static electric field in the ferroelectric [15] and SmC_α^* [14] phases. In both of these phases the conoscopic figure of the uniaxial medium at zero field acquires biaxial characteristics with the optic axial plane *parallel* to the electric field at intermediate fields which then switches to the *orthogonal* direction beyond a critical field [15, 14].

Several models have been proposed to qualitatively describe the transitions between these phases. The above experimental observations, in particular the conoscopic and apparent tilt angle measurements have been interpreted to mean that the Ising type models are more appropriate for the description of these systems. However, no detailed calculations have been made to actually compare with the experimental observations. This motivated us to develop a theoretical model for this system. After taking into account all the physical properties of these compounds and in particular their chirality which leads to helical structures, we developed a model which can be labeled as chiral *Axial Next Nearest Neighbour XY* or *ANNXY* model to describe the various phase transitions exhibited by the antiferroelectric liquid crystals. However, we have not taken into account the transition to the hexatic SmI_A^* phase occurring at lower temperatures in our theoretical model. To test the validity of the basic assumptions of our model, we then theoretically studied the various predictions on the physical properties with and without an external field based on our model and compared them with the relevant experimental observations on these systems.

For AFLC consisting of straight rod like molecules, the chirality of the molecules play an important role for the tilted smectic layers to be polarized in the plane of the layers. However, a polar symmetry of the medium does not require the molecules to be chiral. The necessary condition for a medium to sustain electric polarization is that it has a point symmetry lower than $C_{\infty v}$ which is the symmetry of a polar vector. In fact, recently another liquid crystalline system consisting of bent banana shaped *achiral* molecules has been found to exhibit smectic phases with transversely polarized layers *and* helical structures. We found that our model developed for the AFLC system can easily be adapted to account for the various phases exhibited by this achiral system and their helical structures.

For convenience of discussion, the work is not presented in the above mentioned chronological order. We have first discussed our theoretical studies and the experimental investigations on AFLC which are not yet fully interpreted on the basis of our model are presented in the last chapter.

In chapter 1, we have given a general introduction to some of the liquid crystalline phases which are relevant to the discussions in the later chapters.

In chapter 2, we first discuss the various models proposed so far to qualitatively describe the different phases exhibited by AFLC and their shortcomings. The continuum models [16, 17] first proposed for this system are based on a bilayer order. The experimental observations on the field induced structural changes in the ferroelectric SmC_γ^* and SmC_α^* phases appear to indicate that the assumed bilayer order may not be valid in these phases. On the other hand, *Axial Next Nearest Neighbour Ising* or ANNNI model with third neighbour interaction proposed [18, 19] for this system neglect the basic symmetry of the order parameter for a tilted smectic layer. We believe that the Ising models are inappropriate for the following reasons:

1. From the conoscopic observations it is unequivocally established that all the tilted phases in the absence of field have helicoidal structures of \hat{n} along the layer normal. The assumption of the Ising character of the orientational order parameter within a layer is contrary to these helicoidal structures.
2. It is well known from the theory of ferroelectric liquid crystal (which is also a sub-phase exhibited by AFLC) that the order parameter is a 2-d vector in the plane of the layers, thus indicating xy- rather than Ising- character of the order parameters.
3. Both dielectric and electrooptic measurements detect modes with the relaxation frequencies typical of the Goldstone mode (involving the phase fluctuations of the orientational order parameters). This also indicates an xy-character of the orientational order parameter in these phases.
4. Further even if we assume the ANNNI description as valid, the phase diagrams predicted by these models [20] exhibit a large range of stability of the antiferroelectric $\langle 22 \rangle$ structure as J_1 varies from large positive values in the ferroelectric phase through zero to large negative values in the antiferroelectric phase. However, experimentally this phase is not found in most of the pure compounds and even if it is found in some binary mixtures, it has very short temperature range of stability [6].
5. The ellipsometric studies by Bahr *et al.* [6] have not found any evidence for the 1:2 structure which is predicted by these Ising models to be the structure of the ferroelectric SmC_γ^* phase in the absence of a field.

More seriously none of these models account for the SmC_α^* phase. In order to overcome all the shortcomings of the models described above, we developed a discrete xy-type model.

For molecules within a layer the anisotropic intermolecular dispersion interactions between the cores and end groups of the molecules as well as the packing considerations favour them to be parallel to one another. This gives rise to a strong ferroelectric coupling between the tilted molecules lying *within* a layer. On the other hand, for molecules

in different layers, the interactions are mainly through end groups of the molecules or some long range interactions and are expected to be relatively weak. Therefore, in our discrete model, we assume that the tilt order within the smectic layers arise due to *intra-layer* interactions and such tilted layers are coupled *weakly* through nearest neighbour (NN) and next nearest neighbour (NNN) interactions. As the layers are polarized, one might think that the coupling due to the polarizations may give rise to an antiferroelectric interaction between them. However, as pointed out by Bruinsma *et al.* [21] this interaction is zero in the limit of infinite area of the layers. The anisotropic dispersion interaction between the tilted molecules in adjacent layers favours them to be in a plane which is taken into account by introducing a two fold anisotropic term in the free energy expression in our model. Further, the anisotropic dispersion interaction between the end groups of the molecules favours an antiferroelectric configuration at lower temperatures but the translational entropy gain favours a ferroelectric configuration at higher temperatures. This has been taken into account by introducing a polar interaction between the layers with a temperature dependent coefficient. Bruinsma *et al.* [21] showed that the fluctuations of polarizations of the layers can give rise to a long range antiferroelectric interaction between the layers. To take into account this process in our model, We have introduced a competing antiferroelectric NNN interaction between the layers. From their analysis, we found that this term is expected to be independent of the tilt angle. In addition we have introduced the symmetry allowed chiral interactions between the layers. We have calculated the phase diagram predicted by our model in the appropriate parameter space. The most general phase sequence obtained is: $\text{SmA} - \text{SmC}_\alpha^* - \text{SmC}_\beta^* - \text{FI}_H - \text{FI}_I - \text{FI}_L - \text{SmC}_A^*$, where the symbol FI denotes the ferrielectric phase. Our model correctly takes into account the \mathbf{xy} -character of the order parameter in the tilted smectic layers and for the first time is able to account for the entire sequence of phases exhibited by antiferroelectric liquid crystals. For racemic mixtures or achiral compounds the layers are not polarized and hence the NNN interaction between the layers is zero. In that case all the ferrielectric **as** well **as** the SmC_α^* phases will be unstable **as** seen experimentally.

A number of experiments using static and dynamic electric fields have been conducted on different AFLC systems to elucidate the structures of the different phases. To compare our theoretical predictions with these experiments, **in chapter 3** we have calculated the effect of an external electric field on structures of the different phases. We found that due to the the competition between the inter layer interactions and the field energy various new commensurate structures are stabilized in the presence of a field. At low fields, all the helicoidal structures give rise to the usual soliton lattice structures. In the ferrielectric FI_I and FI_L phases, at intermediate fields a three layer periodic $2/3$ commensurate structure [22] (similar to the $1:2$ structure) is stabilized. In the SmC_α^* phase at intermediate fields a four-layer periodic $2/4$ structure is stabilized. These field induced structures are essential for the interpretation of the various experimental observations. In this chapter, we also calculate an experimentally measurable quantity *viz.* the so called apparent tilt angle as a function of field in the various phases. We found good agreement between experimental and theoretical results. In particular, as mentioned earlier, the plateau at one third of the tilt angle in the variation of apparent tilt angle with field in the ferrielectric phase arises from the field induced $2/3$ structure in this phase.

In chapter 4, we have simulated the conoscopic figures which have been used to

characterize the different phases particularly the ferroelectric phases. From the conoscopic observations in the ferroelectric phase it has been found that the optic axial plane is parallel to the electric field at intermediate fields. This observation has led to the mistaken view in the literature that the xy-type model is not relevant to AFLC. However, we have shown that our xy-type model gives rise to the conoscopic figures which agree extremely well with the experimental observations thus contradicting the above view. In the ferroelectric and the SmC_α^* phases, at intermediate fields, the conoscopic figures with optic axial plane parallel to the field arise from the field induced $2/3$ and $2/4$ commensurate structures stabilized in the respective phases in our model. Another experimental technique which is found to be quite useful in elucidating the structures of the various phases is the ellipsometric study on free-standing films. A number of experiments have been conducted by Bahr *et al.* [23, 24] on the AFLC system. Based on our model, we have also theoretically calculated the temperature variation of the ellipsometric parameters in the absence of a field and compared them with the experimental observations. Again we have found good agreement between the theoretical predictions and experimental observations. For the sake of completeness, we have also calculated the temperature variation of the optical rotatory power in the different phases.

In chapter 5, we have shown that our ANNNXY model for AFLC can be adapted to describe the different phases exhibited by bent *achiral* molecules. Recently Niori *et al.* [25, 26] have synthesized such compounds which exhibit smectic phases, with transversely polarized layers. More interestingly, they found helical structures even in this *achiral* system. Our ANNNXY model accounts for the various phases and the helical structures. The helical structures arise in our model due to the competing interactions between the nearest and next nearest neighbour layers. Since the helical structures are stabilized by spontaneous breaking of the chiral symmetry, both left handed and right handed structures are equally probable. However, due to bent geometry of the molecules there are important differences between the sequence of phase transitions in this system and AFLC consisting of straight rod like molecules.

In Chapter 6, we discuss the results of our electrooptic measurements. When we undertook these experiments there were only a few such measurements and in none of them the antiferroelectric phase was studied due to the small signal in this phase. However, in our experiments we were not only able to get reasonably good signals in the antiferroelectric phase but detected the transition to the lower temperature hexatic SmI_A^* phase which is also antiferroelectric in nature. Our frequency dependent measurements in the ferroelectric, antiferroelectric and SmI_A^* phases show that there are two relaxation modes in these phases. We attribute the high frequency relaxation mode in the antiferroelectric phase to an anti-phase soft mode which can be easily excited by an electric field in this phase.

The future possibilities based on our model presented in this thesis include calculations on the dynamics and the effect of bounding surfaces on the various phases exhibited by AFLC. To summarize

- Our electroptic measurements are able to detect all the transitions between the sub-phases exhibited by antiferroelectric liquid crystals.
- We found an anti-phase soft mode in the antiferroelectric SmC_A^* phase with relax-

ation frequency ~ 100 kHz.

- We have developed a chiral ANNNXY model for AFLC which takes into account the correct symmetry of order parameters in these chiral smectic-C liquid crystals.
- Based on this model, we have calculated the phase diagrams in the appropriate parameter space which for the first time account for all the sub-phases exhibited by AFLC.
- We have studied the influence of a static electric field on the structures of these phases. The field induces new commensurate structures in addition to the usual soliton lattice structures. The variations of the calculated apparent tilt angle with field agree well with the experimental results in different phases.
- We have simulated the conoscopic figures corresponding to these field free and field induced structures. Simulated conoscopic figures agree extremely well with the experiments. Thus the speculation that the xy-model cannot explain the conoscopic figures is incorrect.
- Our simple minded calculations of the temperature variation of ellipsometric parameters exhibit the basic features of the experimental results.
- We have also calculated the temperature variation of the optical rotatory power for this system.
- We have adapted the above model to describe the helielectric transversely polarized smectic phases which were recently discovered in compounds consisting of bent banana shaped chiral molecules.

The following papers contain the works reported in this thesis:

1. S. Sarala, Arun Roy, N. V. madhusudana, H. T. Nguyen, C. Destrad and P. Cluzeau, "Electrooptic Soft Mode Response of Compounds Exhibiting the Antiferroelectric Phase", *Mol. Cryst. Liq. Cryst.*, 261, 1, 1995.
2. Arun Roy and N. V. Madhusudana, "A Simple Model for Phase Transitions in Antiferroelectric Liquid Crystals", *Europhys. Lett.*, **36**, 221, 1996.
3. Arun Roy and N. V. Madhusudana, "Electric Field Induced Structural Transitions in Antiferroelectric Liquid Crystals", submitted to *Europhys. Lett.*
4. Arun Roy and N. V. Madhusudana, "An ANNNXY Model for Transversely Polarized Non-chiral Smectic Liquid Crystals", to be published in *Europhys. Lett.* in press.
5. Arun Roy and N. V. Madhusudana, "A chiral ANNNXY Model for Antiferroelectric Liquid Crystals", to be published.

Chapter 1

Introduction

1.1 Liquid Crystals

The solid, liquid and gaseous phases of matter are manifestations of different arrangements or spatial distributions of the constituent molecules. When the molecules are spherical in shape and the molecular properties are isotropic, the interactions between them will also be isotropic. Therefore, in the phases exhibited by such molecules, one can talk of only the positional order of the centers of mass of the molecules. On the other hand if the shape of the molecules are sufficiently anisotropic, the phases can be characterized by positional as well as orientational order. Thus in a crystalline phase made of such anisotropic molecules, there is a long range positional order of the centers of mass of the molecules as well as a long range orientational order of the principal axes of the molecules. When such a crystalline solid is heated it is not necessary that the break down of these two types of order should occur at the same temperature. Thus, depending on which order breaks down first there are two possibilities:

Plastic crystals: In this case the long range orientational order is broken but the positional order still remains long range. Thus the molecules rotate relatively freely at their respective lattice sites.

Liquid Crystals: In this case the orientational order of the molecules remains long range but the long range positional order of the centers of the molecules is either completely or partially lost.

The liquid crystalline or mesomorphic behaviour was discovered long ago in some compounds consisting of long rod-like organic molecules between their low temperature crystalline phase and the higher temperature isotropic phase. In the recent past, due to their potential applications in display devices, a large number of mesomorphic compounds has been synthesized and a rich variety of liquid crystalline phases have been discovered [27, 28]. The compounds which exhibit such mesomorphic properties as a function of temperature are *thermotropic* in nature. Interestingly, it is found that many surfactant molecules when dissolved in some suitable solvent also exhibit liquid crystalline properties as a function of concentration. This class belongs to *lyotropic* liquid crystals. In this thesis, we will be interested only in thermotropic liquid crystals.

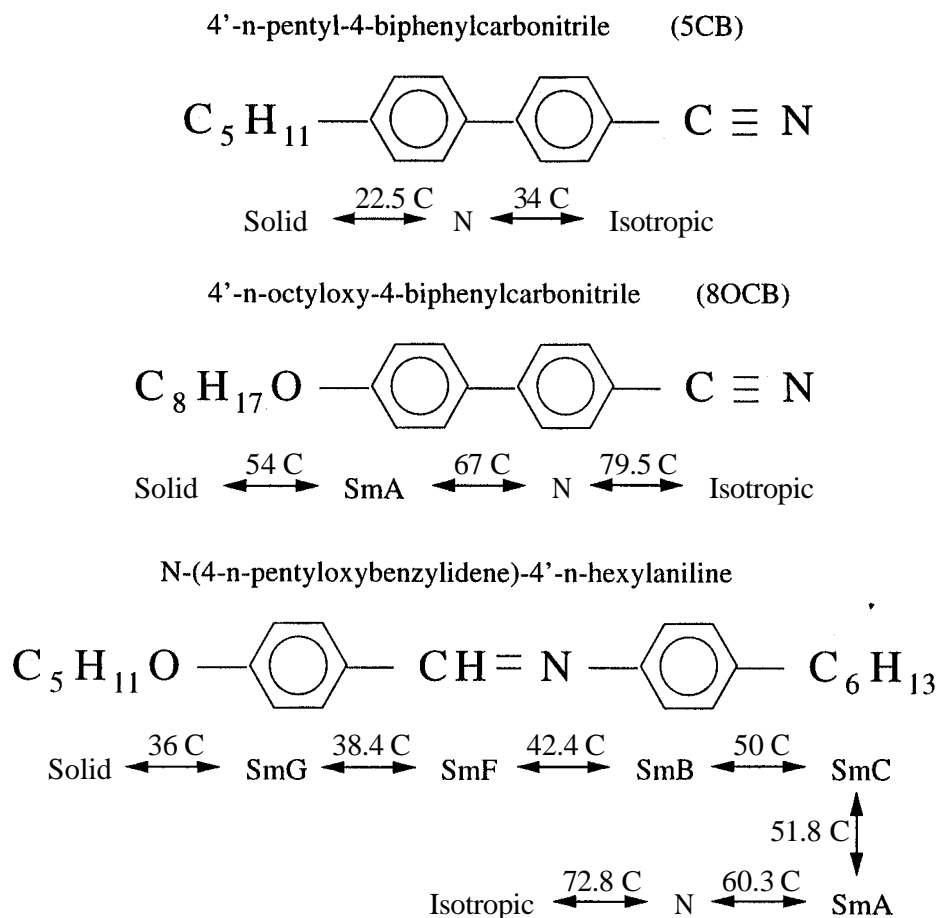


Fig. 1.1: The structural formulae of some of the liquid crystalline compounds and the phase sequences exhibited by them.

The molecular structures of some of the thermotropic liquid crystalline compounds and the phase sequences exhibited by them are shown in Fig. 1.1. Generally these rod-like molecules have a rigid core consisting of benzene or cyclohexane rings and two relatively flexible aliphatic chains at the ends. Further, these molecules can be either *chiral* or *achiral* as discussed below.

1.1.1 Chiral molecules

In general a molecule is said to be *chiral* when its mirror image can not be superimposed onto itself by any operation of translation or rotation. In other words the symmetry group of the molecule does not contain any mirror plane. In addition to the *conformational* chirality which may arise from the conformation or the shape of the molecule, an organic molecule is usually *chiral* when it contains one or more *chiral carbon* atoms. A carbon atom in the organic molecule becomes *chiral* when *all the four groups* bonded to it in the tetrahedral structure are different, otherwise it is *achiral*. There are many conventions in the stereochemistry literature to distinguish the spatial configuration about each chiral

SECTION 1.2

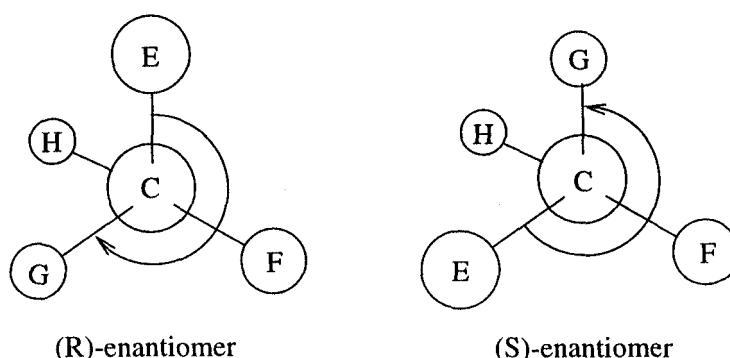


Fig. 1.2: Schematic representation of the spatial configurations of the (R)- and (S)-enantiomers.

carbon atom. In one convention [29], the configurational designation of a chiral carbon atom is obtained by first determining the relationship of the group priorities based on atomic number and certain conversion rule (The Cahn-Ingold-Prelog system). Once the order of the groups is determined, the molecule is held so that the lowest priority group in the sequence is pointed away from the viewer. Then if the other groups, in the order list, are oriented clockwise, the molecule is designated as R (rectus, right), and if anti-clockwise, S (sinister, left). This is illustrated in Fig. 1.2 for the groups (E, F, G, H) in decreasing priority attached to the central carbon atom C.

1.1.2 Achiral molecules

A molecule is *achiral* when the symmetry group of the molecule contains at least one plane of symmetry. In the absence of conformational chirality, an organic molecule is *achiral* when all the carbon atoms in it are *achiral*. However, it should be mentioned here that the presence of chiral carbon atoms in the molecule does not necessarily imply that the molecule is chiral. An even number of chiral carbon atoms present in the molecule may cancel chiral effects of each other to make the molecule as a whole achiral.

1.2 Nematics

The most common and simplest liquid crystalline phase exhibited by these long anisotropic organic molecules is the nematic phase. In this phase there is no long range positional order between the centers of mass of the molecules but the long axes of the rod-like molecules are on average oriented along a common direction. In other words the positional distribution function of the centers of mass of the molecules is spatially uniform but the orientational distribution of the axes of the molecules is anisotropic. Depending on the chirality of the constituent molecules, one obtains two types of phases with the above characteristic distributions *viz.* the *nematic* phase when the molecules are *achiral* and the *cholesteric* phase when the molecules are *chiral*. We will briefly describe below these two phases. A detailed discussion of the properties of these phases can be found in the book by de

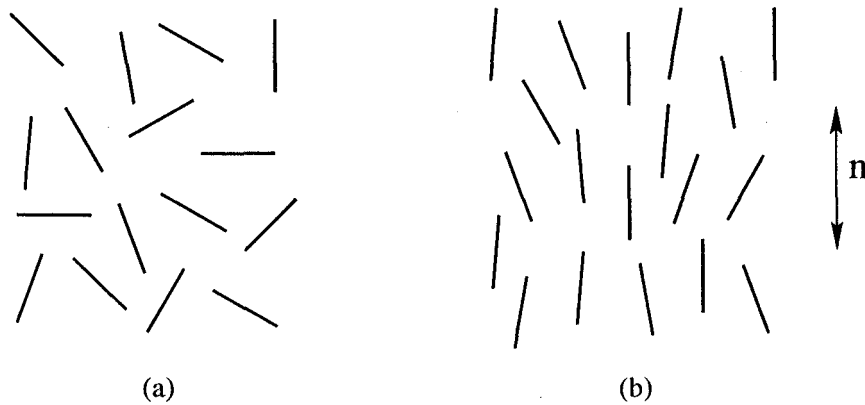


Fig. 1.3: Schematic representation of the arrangement of rod like molecules in the (a) isotropic and (b) nematic phases.

Gennes [27].

1.2.1 Nematic phase (N)

A schematic representation of the orientational order in a nematic liquid crystal is shown in Fig. 1.3b. In this phase the rod-like *achiral* molecules are on average aligned with their long axes parallel to each other and the orientational order is uniform in space in an ideal sample. The correlation between the centers of mass of the molecules is similar to that in conventional liquids, apart from the anisotropy in the correlation length. Thus nematics flow like liquids though the flow is relatively viscous. To describe the local direction of alignment of the molecules, one usually defines a unit vector \hat{n} , called the director, which gives at each point in the sample the direction of the preferred axis of orientation. The states described by A and $-A$ are indistinguishable even if the constituent molecules are *polar* and hence A is *apolar* (*i.e.*, $A \leftrightarrow -\hat{n}$ symmetric) in nature. Optically this medium is uniaxial positive with the largest principal refractive index along \hat{n} and having the macroscopic point symmetry $D_{\infty h}$. Thus nematic liquid crystals are birefringent and this property is exploited in display devices.

In order to define a nematic order parameter, following De Jeu [30], let us make the simplifying assumption that the molecules are rigid rods. To define the local orientation of the long axes of the molecules at a point $\vec{r} = (x, y, z)$ we attach to the rod a unit vector \hat{a} along the long axis. Now consider the thermal averages of the relevant tensors that are composed of \hat{a} , over a small but macroscopic volume around \vec{r} . The first choice is a vector order parameter $\langle \hat{a} \rangle$, where the angular brackets denote the ensemble average. This is analogous to the magnetization in a ferromagnet. However, a nonzero value of this order parameter would violate the equivalence of \hat{n} and $-A$. It would describe a polar nematic phase that has not yet been observed.

The next choice as order parameter is a second rank tensor S , the elements of which are given by

$$S_{\alpha\beta} = \langle a_{\alpha}a_{\beta} \rangle - \frac{1}{3}\delta_{\alpha\beta}, \quad \alpha, \beta = x, y, z. \quad (1.1)$$

Note that the addition of the Kronecker delta ensures that $S_{\alpha\beta}$ is zero in the isotropic phase where $\langle a_\alpha^2 \rangle = 1/3$. The tensor order parameter S is symmetric and traceless and thus has in general five independent elements. By choosing a suitable coordinate system (principal coordinate system) such a tensor can always be brought to a diagonal form. For the uniaxial case, denoting the average direction of alignment of the molecules by the director \hat{n} , the most general form of the order parameter field in the nematic phase is given by

$$S_{\alpha\beta}(\vec{r}) = S(n_\alpha(\vec{r})n_\beta(\vec{r}) - \frac{1}{3}\delta_{\alpha\beta}), \quad (1.2)$$

where the scalar S is a measure of the degree of alignment of the long axes of the molecules along $\hat{n}(\vec{r})$ and the expression in the parenthesis takes care of the spatial variation of $\hat{n}(\vec{r})$ from point to point. In a well aligned nematic, \hat{n} is independent of \vec{r} .

1.2.2 Chiral nematic or cholesteric phase (N^*)

If the compound exhibiting the nematic phase is doped with a chiral dopant or the molecules themselves are chiral, the nematic phase in general is not thermodynamically stable. The stable thermodynamic phase one obtains in this case is the cholesteric phase (N^*). Locally this phase is like the nematic phase. However, because of the inherent chirality of the medium, the director \hat{n} is no longer constant in space but forms a helical super structure. If the helix axis is taken to be along the z-axis, the equilibrium configuration of the director \hat{n} in this phase can be written as

$$n_x = \cos(qz), \quad n_y = \sin(qz), \quad n_z = 0, \quad q = 2\pi/p, \quad (1.3)$$

where p is the temperature dependent equilibrium pitch. A schematic representation of the structure of the cholesteric phase is shown in Fig. 1.4. Due to the equivalence of \hat{n} and $-\hat{n}$ the repeat distance or the physical periodicity in this phase is defined as the distance along the helical axis over which \hat{n} turns by π which is $p/2$. The inherent chirality of the constituent molecules forbids the medium to have a plane of symmetry and the medium is characterized by the point symmetry D_2 .

1.3 Smectics

In smectic phases in addition to the orientational order of the long axes of the molecules there is a one dimensional quasi-long range positional order of the centers of mass of the molecules. This one dimensional periodic modulation of the density (taken along the z-axis) can be described in a Fourier series

$$f(z) = \sum_{n=0}^{\infty} a_n \cos(2\pi n z/d), \quad n \text{ integer}, \quad (1.4)$$

where the coefficients a_n are determined by averaging the relevant cosine-functions over the positional distribution function $f(z)$. Restricting the expansion to the first harmonic only, one arrives at the smectic order parameter

$$\rho = \int f(x) \cos(2\pi z/d) dz = \langle \cos(2\pi z/d) \rangle. \quad (1.5)$$

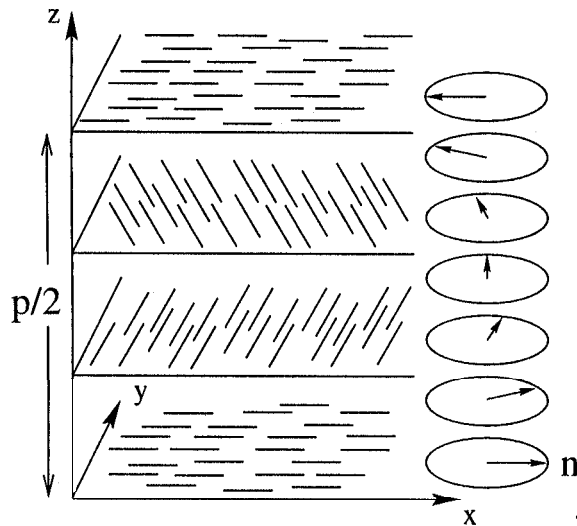


Fig. 1.4: Schematic representation of the helical structure of the director \hat{n} in the cholesteric phase consisting of chiral molecules. Though \hat{n} is represented by an arrow in the figure, it is actually apolar in nature.

Smectic liquid crystals are described as a stacking of fluid layers. However, as the density modulation is only one dimensional, the thermal fluctuations of the layers are subjected to the Landau-Pierls instability according to which the thermal fluctuations of the layers diverge logarithmically with the sample size. As such, it is quite adequate to take only the first harmonic in the Fourier expansion given by Eq. 1.4. Depending on the orientation of the nematic director \hat{n} with respect to the wave vector of the one dimensional density modulation, smectic liquid crystalline phases can be of the following types:

1.3.1 Smectic A phase (SmA)

In the smectic A or SmA phase, the one dimensional density modulation is along the director A. Therefore, roughly speaking the SmA phase consists of a stack of fluid layers in which the director \hat{n} is parallel to the layer normal. The layer thickness is approximately equal to the length of the molecules as shown in Fig. 1.5a. The medium is positive uniaxial with the point symmetry $D_{\infty h}$ which is the same as that of nematic. The additional space symmetry is the discrete translational one *viz.* T_1 .

1.3.2 Smectic C phase (SmC)

The characteristic property that distinguishes the SmC from the SmA phase is that in the former the director \hat{n} is tilted with respect to the layer normal. The schematic representation of the SmC type of order is sketched in Fig. 1.5b. Firstly within a layer \hat{n} is uniformly tilted by an angle θ with respect to the layer normal. Secondly the tilt directions of the various layers are correlated. Thus the tilted orientational order can be described by a two dimensional vector *viz.* the so called c-director \vec{c} which is the projection of \hat{n} on the

SECTION 1.3

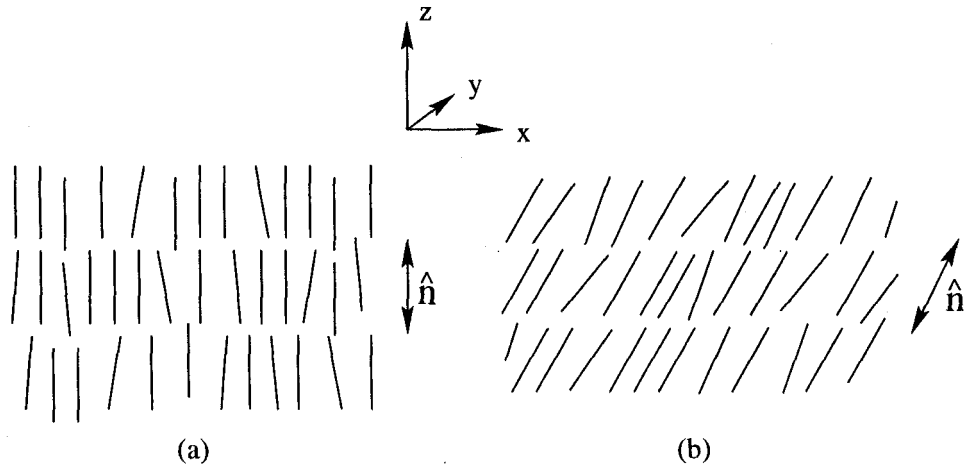


Fig. 1.5: Schematic representation of the order of rod like molecules in the (a) smectic A (SmA) and (b) smectic C (SmC) liquid crystals.

layer plane. The correlation of the tilt directions of different layers implies that \vec{c} must be uniform over macroscopic distances. Clearly the SmC phase is still $A \leftrightarrow -\hat{n}$ symmetric. However such a symmetry operation does not hold for the c-director. The states described by Z and $-\vec{c}$ are not equivalent and hence \vec{c} is a 2-d polar vector. The tilted structure in SmC introduces biaxiality within the layers and SmC is optically biaxial with point symmetry C_{2h} . Due to the tilted orientation of the director A, the layer thickness $d \approx l \cos \theta$, where l is the length of the molecules. In general the tilt angle θ varies with temperature and depending on the nature of the higher temperature phase there are two broad classes of SmC materials. The majority form the SmC phase by cooling from the SmA phase through a second order transition and show a tilt angle which increases from 0° as the temperature is decreased from the SmA-SmC transition temperature. However, in some compounds the SmC phase appears by a first order phase transition as the sample is cooled from either nematic or isotropic phase. In this case the layers with tilted molecules have to appear directly at the transition, which makes the transition usually first order in nature and the tilt angle is usually large and practically independent of temperature.

1.3.3 Chiral smectic C phase (SmC*)

In the layer level, the only fundamental difference between the SmC and SmC* phases is that the layers in the SmC* phase lack the mirror plane symmetry. Thus, the SmC* phase can be obtained in several ways — for instance, by synthesizing a chiral variant of a molecule which is known for its stable SmC phase, or by doping a SmC liquid crystal with any chiral compound soluble in it: symbolically, $\text{SmC} + \text{*} \rightarrow \text{SmC*}$.

As in the SmC phase, the director A is tilted with respect to the layer normal. In each layer the c-director is uniform. However, unlike in the SmC phase, due to the inherent chirality of the medium, \vec{c} forms an uniform helical structure along the layer normal. A schematic representation of the structure of the SmC* phase is shown in Fig. 1.6. The chirality of the molecules removes the mirror plane from the symmetry group C_{2h} of the

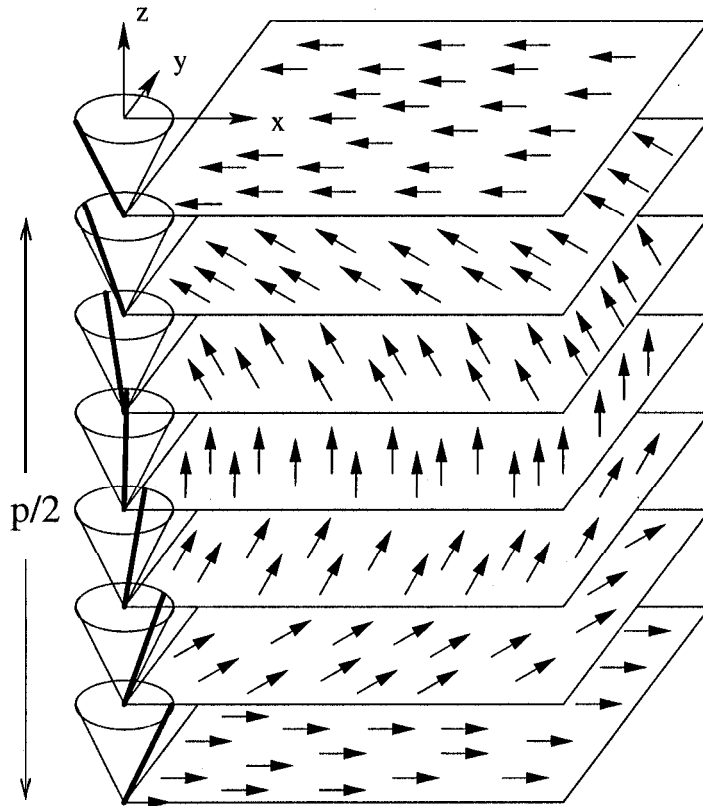


Fig. 1.6: Schematic representation of the structure in the ferroelectric SmC^* phase. The arrows indicate the projection of the director \hat{n} on the smectic layers (\vec{c} -director) which has a helical structure along the layer normal. Note that the angle between the \vec{c} vectors in successive layers (which is usually $\sim 1\text{--}2^\circ$) has been highly exaggerated for clarity.

SmC phase and the local point symmetry of the SmC* layer is C_2 . With a profound insight Meyer *et al.* [1] first demonstrated that this lower symmetry of the SmC* layers allows them to be transversely polarized along the C_2 axis and hence SmC* is also referred to as a ferroelectric liquid crystal. However, because of the helical precession of the director \hat{n} and thus the polarization about the layer normal, a more correct denomination is *helielectric* liquid crystal. Unlike the cholesteric phase, as \vec{c} and $-\vec{c}$ are not equivalent in this case, the physical periodicity is the distance over which \vec{c} turns by 2π i.e., the full pitch p . Since the layer polarization is associated with a tilt of the director \hat{n} , SmC* liquid crystals have potential application in display devices. This has led to synthesis of a large number of compounds exhibiting the SmC* phase. The structure and properties of this liquid crystalline phase have been studied in great detail (see the book by Goodby *et al.* [31] for a review).

1.3.4 Chiral smectic C antiferroelectric liquid crystals

In addition to the ferroelectric phase in the SmC* liquid crystals which is now quite well understood, Chandani *et al.* [2] in 1989 discovered antiferroelectric properties in the smectic phase exhibited by the compound MHPOBC. Since its discovery various experimental studies revealed that in addition to the antiferroelectric (SmC*_A) phase, this novel compound exhibits a variety of other phases. The phase sequence for the prototype compound MHPOBC with decreasing temperature is:

$$\text{SmA} - \text{SmC}^*_\alpha - \text{SmC}^*_\beta - \text{SmC}^*_\gamma - \text{SmC}^*_A - \text{SmI}^*_A - \text{Cryst.}$$

The SmC*_ β phase in the so called bookshelf geometry exhibits bistable switching when a triangular wave voltage is applied across the cell and is identified with the usual ferroelectric SmC* phase discussed above. However, the lower temperature SmC*_A phase in the same geometry exhibits a trilevel switching when the amplitude of the triangular wave is sufficiently large and is characterized as antiferroelectric in nature. The structure of this antiferroelectric SmC*_A phase established by various experimental techniques [2, 3, 4, 5] is the following:

The director \hat{n} in this phase like in the SmC* phase is uniformly tilted with respect to the layer normal. However, unlike in SmC* phase, the difference in azimuthal angle of \hat{n} in successive layers is $\pi + a$. The small angle a gives rise to a helical structure of \hat{n} along the layer normal and arises from the chirality of the constituent molecules. The sign of a is determined by the handedness of the enantiomer. Thus the equilibrium director configuration in this phase taking the layer normal along the z-axis is

$$n_{kx} = \sin \theta \cos(k\psi), \quad n_{ky} = \sin \theta \sin(k\psi), \quad n_{kz} = \cos \theta, \quad (1.6)$$

where $\psi = \pi + a$ and n_{kx}, n_{ky}, n_{kz} denote the Cartesian components of the director \hat{n} in the k-th layer. The tilt angle θ is uniform and usually depends on temperature. As the polarization of the layer is along the C_2 axis, it is clear that the polarization in successive layers is nearly opposite giving rise to the antiferroelectric property. A schematic representation of the ordering of \hat{n} in different layers is shown in Fig. 1.7. It should be pointed out that the smectic-O phase discovered by Levelut *et al.* [32] by x-ray studies on the compound MHTAC was later confirmed by Galerne *et al.* [4] to be the antiferroelectric

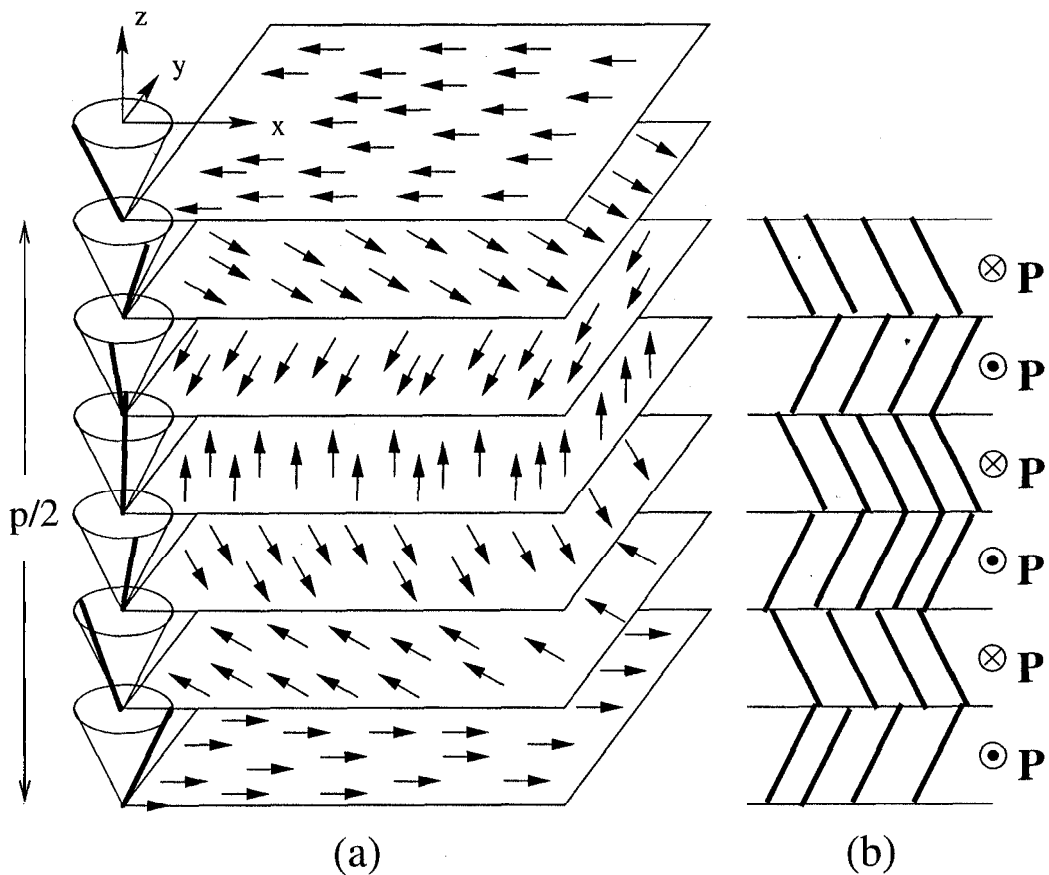


Fig. 1.7: Schematic representation of the structures in the antiferroelectric SmC_A^* phase: (a) Bulk helical structure. The arrows indicate \vec{c} vectors within the layers which have a helical structure along the layer normal. Note that the angle between the \vec{c} vectors in successive layers is close to π . The deviation from π has been highly exaggerated for clarity in the diagram. (b) Unwound herringbone structure. \mathbf{P} denotes the polarization of the of the layers.

SmC_A^* phase. Though the structure of SmC_A^* phase is known, the structures of the SmC_γ^* phase as well as the SmC_α^* phase are not yet clearly established. From the polarization measurements, SmC_γ^* phase is characterized as ferrielectric in nature as its polarization is less than that of the ferroelectric SmC_β^* phase. The SmC_α^* phase appears just below the stability range of the SmA phase and has a small tilt angle and a very short pitch. As the main part of this thesis work is based on studying the properties of these fascinating liquid crystalline phases, we will discuss their properties in detail in the following chapters. For a review of this subject reference may be made to Fukuda *et al.* [6].

Though antiferroelectric liquid crystals (AFLC) are known since 1989, the theoretical as well as the experimental understanding of this novel liquid crystalline system is not complete. On the experimental side, as mentioned above, the structure of the antiferroelectric (SmC_A^*) phase is clearly known but despite a number of experimental attempts, the structures of the ferrielectric SmC_γ^* phase as well as the SmC_α^* phase are not yet clearly established. On the theoretical side, various phenomenological models have been proposed to qualitatively describe the properties of some of the phases but none of the models proposed so far is able to account for all the phases exhibited by this system and further the inherent assumptions of the models are quite unsatisfactory. In Chapter 2 we will describe a model developed by us to account for the entire sequence of phases for the first time. Our model correctly takes into account the basic symmetry of the smectic layers and can be labeled as a chiral *Axial Next Nearest Neighbour XY* (ANNNXY) model. In chapter 2 we will also describe the structures of the different phases and the phase diagrams predicted by our model and compare them with the experimental results and other relevant models.

As we have mentioned above, a number of experiments have been conducted on this system to elucidate the structures of the different phases. Since the medium is polarized, the experiments often involve applying a static or dynamic electric field to study the resulting changes in the structures of the different phases. In most of the experiments, the changes in the structure are usually probed using polarized light. In Chapter 3 we have studied the influence of an externally applied static electric field on the structures of the different phases predicted by our model. We find that new commensurate structures are stabilized by the field which originate from the competing interactions between the layers and the field energy. We also calculate an experimentally measurable quantity *viz.* the so called "apparent tilt angle" to compare our results with the experimental observations.

Among the various optical measurements made on this system, two measurements *viz.* conoscopic and ellipsometric studies are found to be quite useful in elucidating the structures of the different phases. Therefore, in Chapter 4, we have simulated the conoscopic figures corresponding to the field free and field induced structures predicted by our model in the different phases. We have also calculated the ellipsometric parameters and optical rotatory power in the different phases to compare with the experimental observations. We find that the theoretical predictions agree reasonably well with the experimental observations. This implies that the basic ingredients of our model are quite appropriate for the description of the structures exhibited by antiferroelectric liquid crystals.

We have also made some electrooptic measurements on this system. In fact we started our investigations on the AFLC compounds experimentally to characterize the different phases by electrooptic measurements. We found that these measurements could be used

to detect the different transitions. At that stage, we found that there was no satisfactory theory to account for all the phases seen experimentally. This motivated us to develop the chiral ANNNXY model for this system which constitutes the major part of this thesis. However, for the interpretation of our electrooptic measurements, the appropriate dynamical equations based on our model taking into account the viscous and elastic properties of the phases have to be solved. We have not yet taken up this exercise. In Chapter 6 we have discussed the experimental observations and the relaxation frequencies obtained from our electrooptic measurements.

The AFLC system consisting of straight rod like molecules requires the latter to be chiral for the layers to be transversely polarized. However chirality of the molecules is not an absolute necessity for the layers to be polarized. In fact, recently smectic liquid crystals consisting of *achiral* bent banana shaped molecules have been found to exhibit such transverse polarization. In Chapter 5 we will describe this system and show that our ANNNXY model can be adapted to describe the various phases exhibited by the banana shaped molecules.